Astron. Astrophys. 339, 525–530 (1998)

ASTRONOMY
AND
ASTROPHYSICS

On the origin of shock waves in the β Cephei star BW Vulpeculae*

P. Mathias[1], **D. Gillet**[2], **A.B. Fokin**[2,3], **and T. Cambon**[1]

[1] Observatoire de la Côte d'Azur, Département Fresnel, UMR 6528, BP 4229, F-06304 Nice Cedex 04, France
[2] Observatoire de Haute-Provence, F-04870 St Michel l'Observatoire, France
[3] Institute for Astronomy of the Russia Academy of Sciences, 48 Pjatnitskaja, 109017 Moscow, Russia

Received 3 July 1998 / Accepted 12 August 1998

Abstract. New high temporal and spectral resolution observations of BW Vul are presented. The line doubling phases, occurring twice per pulsation cycle during the velocity discontinuities, are interpreted in terms of shock waves. The first and largest doubling is seemingly due to the formation of a shock wave during the supersonic infalling motion of the atmosphere. The famous observed stillstand would be only the last phase of the ballistic motion which seems marked by a small bounce of the atmospheric layers on the photosphere. Then, a new shock wave, probably initiated by the iron κ-mechanism, sweeps the layers upward. There is some indications that the amplitude of the motion of atmospheric layers changes from one pulsation cycle to another one.

Key words: line: profiles – shock waves – stars: individual: BW Vulpeculae – stars: oscillations

1. Introduction

The star BW Vul has the largest amplitude (about 200 km.s^{-1}) among the known β Cephei stars. This class is found to be destabilized by a κ-mechanism acting in the metal opacity bump, near $T \sim 2\,10^5$ K (e.g. Cox et al. 1992, Dziembowski & Pamyatnykh 1993). However, this usually leads to relatively small amplitude (of the order of 20 km.s^{-1}) with slow line profile variations, often interpreted in terms of non-radial modes. On the contrary, BW Vul presents a complex velocity curve, with two discontinuities during each pulsation cycle, surrounding a nearly constant velocity phase called stillstand. These two abrupt velocity changes are followed by a phase of line doubling, while at other phases the profiles remain more or less symmetric.

Physically, a line doubling phenomenon is associated with either a non-radial mode (linear theory) or a shock wave (nonlinear theory). Non-radial modes for BW Vul have already been invoked (Kubiak 1978, Odell 1981). However, the moment method (Aerts 1996), based on the linear pulsation theory as the above studies, favored a radial mode, instead of a non-radial one, (Aerts et al. 1995) which cannot reproduce a line doubling. Conversely, a shock wave propagation can induce such a profile as suggested by Schwarzschild (1954) for W Virginis stars.

First, Odgers (1955) invoke for BW Vul an upper atmosphere accelerated by non-linear radial pulsations, involving a shock wave which impulsively separates this layer from the photosphere, becoming a shell. When the shell falls back, a decrease in its optical thickness occurs, allowing to see the "static" photosphere: two line components are thus present, one being at the systemic velocity, the other one being redshifted. The origin of the same shocks is different for Crowe & Gillet (1989). Indeed, in their scenario, there are two κ-mechanism acting: the one associated to the first discontinuity involves the propagation of a shock wave, coming from the inner part of the star, which appears during the infalling motion of the atmosphere. The other one, as in the case of Odgers (1955), deals with the impulsion mechanism, and concerns the second discontinuity.

Other explanations have been proposed as well. Young et al. (1981) suggest that a stationary layer is generated during the infalling atmospheric motion by the strong temperature and gas pressure increases. Thus a line doubling phenomenon appears. Recently, using a nonlinear pulsational model, Moskalik & Buchler (1994) found that the stillstand is caused by an outward propagating shock which originates at the bottom of the He II ionization zone. The consecutive strong compression provokes a sudden jump of the Rosseland-mean opacity which contributes to the formation of an apparent discontinuity in the observed radial velocities. Nevertheless, their solution shows that the stillstand is at a radial velocity of -100 km.s^{-1} in the stellar rest frame while it is now well established by accurate spectral observations that it is close to a zero velocity.

These pictures are not equivalent, and it is the aim of this paper to try to select the best model. The observations are described in Sect. 2 and the line doubling phenomena are discussed in Sect. 3. The origin of the two shock waves and the sketch of the cycle are proposed in Sect. 4. Finally, some concluding remarks are given in Sect. 5.

2. Observations and data reductions

The observations were carried out with the cross-dispersed spectrograph ELODIE (Baranne et al. 1996). This instrument is at

Send offprint requests to: P. Mathias

* Based on observations obtained at the Observatoire de Haute Provence (France)

the Cassegrain focus of the 1.93 m telescope of the Observatoire de Haute-Provence. The detector was a thinned Tk-CCD, with 1024×1024 elements of size 24 μm^2.

The observations were obtained during two nights, namely August 1$^{\rm st}$ and 8$^{\rm th}$, 1994. The spectral domain ranges from 3900 Å to 6800 Å with a resolving power of 42 000. The typical exposure time was 6 min, leading to a signal-to-noise ratio around 50 for the lines considered in this paper (essentially $\lambda\lambda$ 4553 Si III and Hα lines). We reduced the spectra with the INTER-TACOS software (Baranne et al. 1996) that takes care of the offset and flat-field pixel-to-pixel corrections. Finally, the spectra were normalized to the continuum using a cubic spline function and computed in the heliocentric frame.

Approximately, each night represents 1.2 pulsation cycle ($P = 4$ h 50 mn). The pulsation phases φ were computed using the ephemeris given by Odell (1994):

$$\text{HJD} = 2\,447\,700.1158 + 0.201044444\,\text{d}.$$

3. Line doubling phenomena

The most important observationnal characteristic of BW Vul is the presence of two line doubling phenomena which occur at each velocity discontinuity. Fig. 1 represents a series of spectra before and after the stillstand.

To interpret these line profiles, it is important to compute the spectra in the stellar rest frame i.e., the systemic velocity γ of the star must be calculated. This is usually done by an integration of the velocity curve over one pulsation period. But this supposes that the shape of the radial velocity curve is well determined i.e., the number of spectra is large enough. Because at some phases a line doubling appears, three kind of velocities can be measured. First, when they are visible, we can fit each line component (the blueshifted and the redshifted ones) by a gaussian to obtain their velocity (Fig. 2a) or a single gaussian fit over the whole profile whatever its shape (Fig. 2b).

Contrary to the double gaussian fit, only the single one provides a mean velocity of the motion of the atmospheric layers. The physical meaning of this average velocity is weakly informative on the dynamics of the atmosphere. Thus, the γ-velocities which can be deduced from these three velocity curves (Fig. 2a and b) are quite different. It is around -20 km.s^{-1} for the blue component, 4 km.s^{-1} for the red one and -11 km.s^{-1} for the whole profile. For the second night (August 8$^{\rm th}$), we respectively find -14 km.s^{-1}, 1 km.s^{-1} and -10 km.s^{-1}.

At phase $\varphi = 0.55$, the Si III line profile has the more symmetrical and narrow shape and hence can be interpreted as the phase of the largest atmospheric extension, when the velocity field within the line formation region may be negligeable. Thus, its associated radial velocity (- 7.6 km.s^{-1}) can be considered as close to the systemic velocity. For the night August 8$^{\rm th}$, we obtained -10.8 km.s^{-1}. Thus, we have assumed hereafter that the systemic velocity of BW Vul can be estimated by the average of these two evaluations over our two observation nights. The adopted value -9.2 ± 1.7 km.s^{-1} was used to compute the spectra in the stellar rest frame. This value is not very different from the average (-10.5 km.s^{-1}) of the γ-velocities for the whole profile.

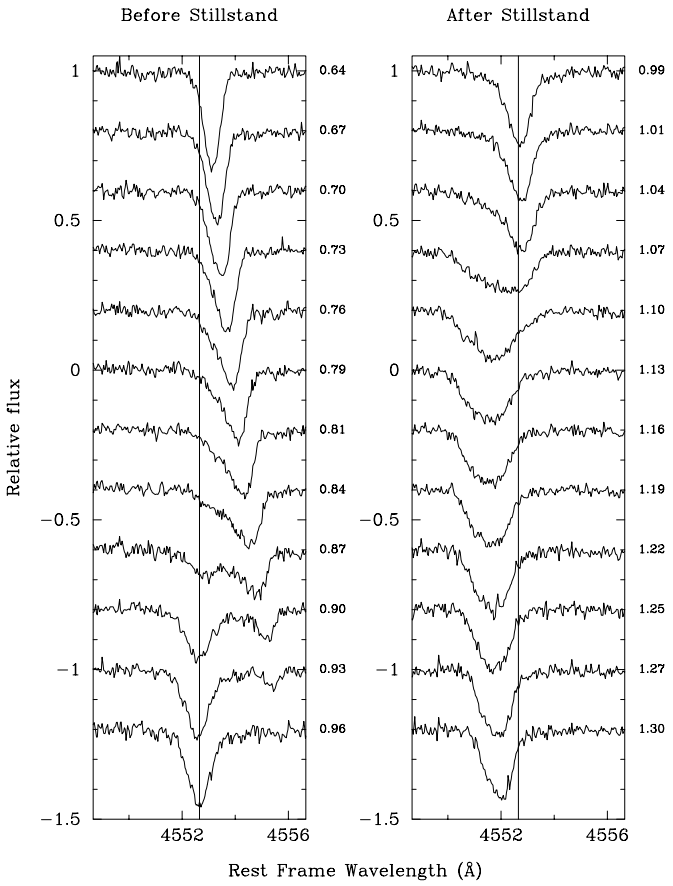

Fig. 1. Spectra of the $\lambda\lambda$ 4553 Si III line for the night August 1$^{\rm st}$, 1994. The pulsation phase φ is given on the right of each spectrum. The left column concerns spectra obtained during the first velocity discontinuity (maximum inward atmospheric motion), whereas the right column displays spectra during the second discontinuity (maximum outward velocity). The spectra are computed in the stellar rest frame (see text), the vertical line representing the laboratory wavelength

Our spectra follow the same general pattern as previous observations. During the inward atmospheric motion, the profile becomes slightly asymmetric ($\varphi = 0.67$) on the blue side and then more and more complex, until two components can be clearly distinguished ($\varphi = 0.87$). In the meantime, the red component decreases until disappearing ($\varphi = 0.96$). Note that the blue component is slightly redshifted until $\varphi = 0.87$, while it is close to a zero-velocity at $\varphi = 0.90$, 0.93 and 0.96. If the red component is considered alone, it seems to be more and more redshifted, regularly, during the whole spectra set. One can easily imagine a straight line joining the cores, at the different phases.

This behavior is similar after the stillstand, except that the doubling is not resolved and is much shorter (between $\varphi = 1.04$ and 1.07). However, this time, the blue component is really blueshifted and the red one is at zero-velocity. Then, from $\varphi = 1.10$ to $\varphi = 1.16$, the profile is symmetric, and blueshifted. Finally, from $\varphi = 1.16$ until $\varphi = 1.30$, the profile slowly moves

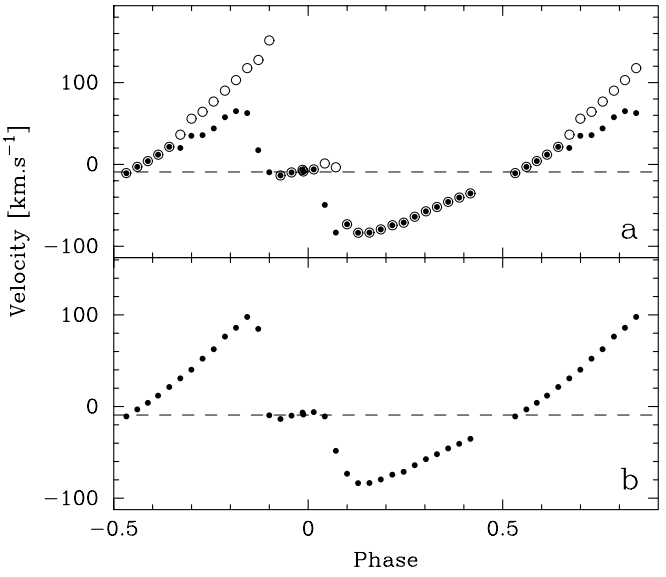

Fig. 2a and b. Heliocentric radial velocity curves as a function of pulsation phase. **a** Velocites associated respectively to the blue (dots) and the red (circles) line components. **b** Mean velocity curve, obtained with a single gaussian fit over the whole profile whatever its shape. In both cases, the horizontal dashed line represents the γ-velocity axis

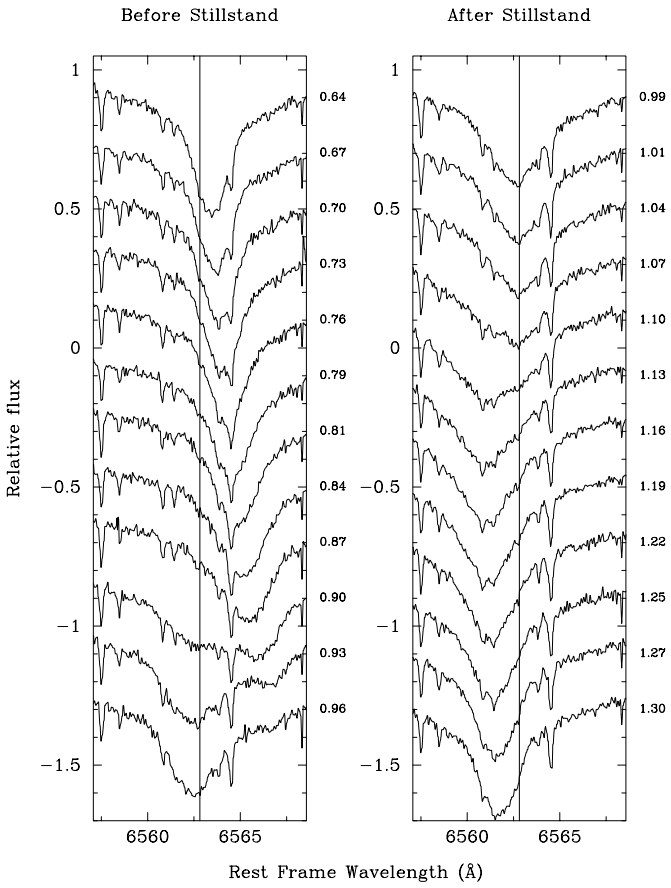

Fig. 3. Same as Fig. 1, but for the Hα line. Note that the velocity scale ($\Delta\lambda/\lambda_0$, where λ_0 is the laboratory wavelength) is the same as in Fig. 1. The constant small absorptions present through the profile are caused by telluric H_2O lines

to the red and becomes more and more sharper. This is well illustrated on Fig. 2a: from $\varphi = 0.15$ to 0.64, the velocity curve is smooth. Then, the asymmetric profile can be fitted with two gaussians, providing for both components an increasing velocity, the red component being in the continuity of the velocity curve, while the blue component decelerates.

When the two components are visible, the blue curve undergoes the first discontinuity which shifts the velocity to zero by 70 km.s^{-1}, while the red curve vanishes at $\varphi = 0.96$, inducing a gap of about 180 km.s^{-1}. Moreover, it appears that the stillstand is not really constant, the velocity, after a very short expansion, being slightly positive. Then the second doubling induces the second velocity discontinuity, affecting first the blue component, with a gap around 80 km.s^{-1}. After this violent expansion, the velocity seems to follow a ballistic motion.

This behaviour is nearly, but not exactly, the same in the upper atmosphere where Hα is formed. Indeed, because the Si III line has a larger ionization and excitation potential compared to that of Hα, it is thought to be formed lower in the stellar atmosphere (see Sect. 4). Hence, the physical conditions may be different between the two line formation regions. Fig. 3 represents, for the same phases as Fig. 1, the Hα spectra. Of course, the Hα profile being very broad, it is not as easy as in the case of the Si III line to appreciate at which phase the profile becomes asymmetric, and even to distinguish the line doubling components. Only spectra at $\varphi = 0.90$ and 0.93 show such an evidence. Furthermore, the second doubling phase can only be suspected at $\varphi = 1.10$. However, it seems that the amplitude of the doubling phase is comparable for both Si III and Hα lines. The only difference between them is that the doubling discussed above for the Si III line happens slightly later for the Hα one ($\Delta\varphi \simeq 0.03$).

We have compared these spectra with those obtained on night August 8$^{\rm th}$ which are represented, for the Si III line, on Fig. 4. The most striking difference between the two nights is that the line doubling is poorly seen during the second night. This is particularly true on phase $\varphi = 0.89$. Also, during the first discontinuity, the spectra obtained on August 8$^{\rm th}$ are much more symmetric (until $\varphi = 0.74$). The same velocity curves as in Fig. 2a and b are displayed in Fig. 5a and b. One can see that the red curve is not a straight line as in Fig. 2a and b but decelerates at nearly the same amount as the blue one. During the first velocity discontinuity, the velocity jump associated to the red curve is about 130 km.s^{-1}, and that associated to the blue curve is around 70 km.s^{-1}. As for the second velocity discontinuity, the gap is larger for the red component, being around 100 km.s^{-1}.

4. Shock wave origins

As said in the previous section, the maximum extension of the atmosphere occurs at $\varphi = 0.55$. After this phase, the layers start their infalling motion due to gravity. In the absence of opposite

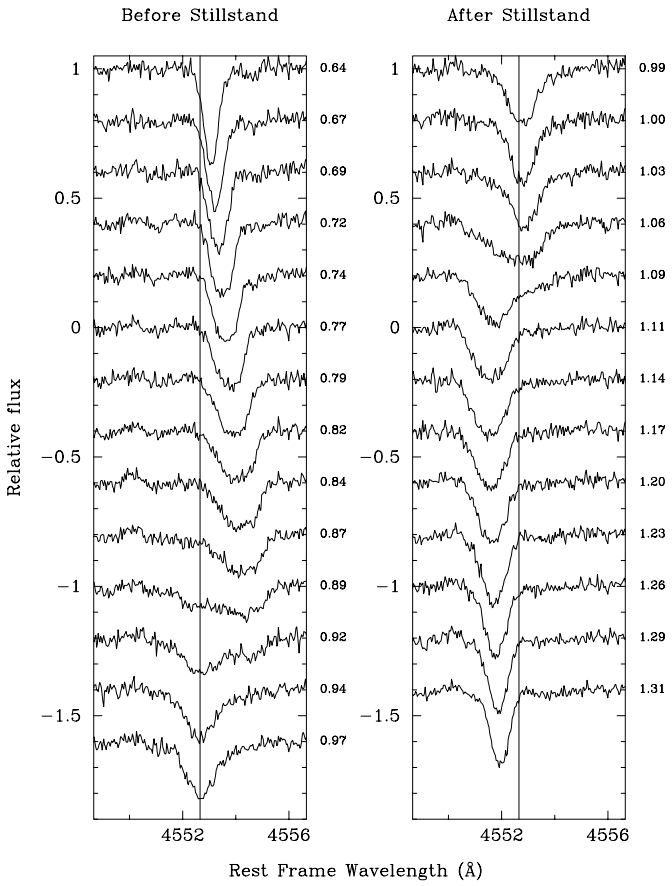

Fig. 4. Same as Fig. 1, but for the night August $8^{\rm th}$

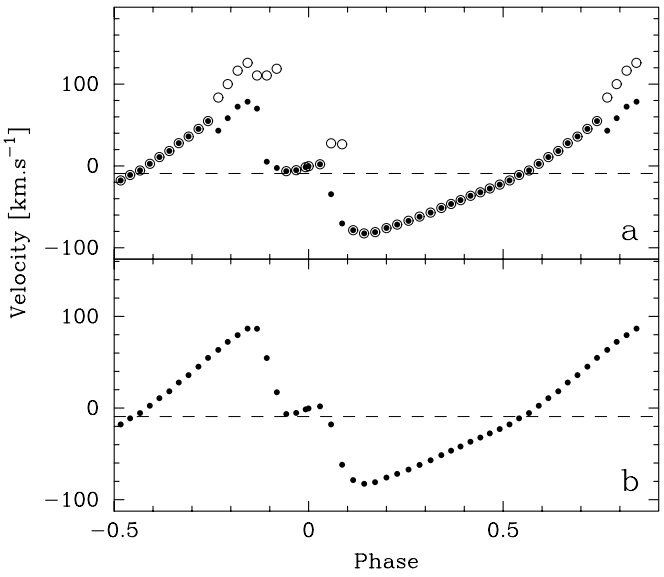

Fig. 5a and b. Same as Fig. 2, but for the night August $8^{\rm th}$. Note that axis scales are the same as in Fig. 2

forces (small density gradients or radiation pressure), the atmosphere would be continuously accelerated. This is in accordance with the motion of the red core component during the largest discontinuity, which can be represented by a straight line (Fig. 2a). In this case, the slope of this line (about 29 m.s^{-2}) should approximately corresponds to the gravity of the star. As for the blue component, the associated deceleration is much lower, being around 20 m.s^{-2}. Therefore, there is a mechanism which stops the free fall motion. Indeed, when the bottom of the layer is falling, it encounters the deepest photospheric layers which are denser. Consequently, a strong pressure gradient develops between the bottom and the top of the line formation region. This gradient becomes so large ($\varphi = 0.87$) that the induced compression wave front breakes into a shock wave. Indeed, at this phase, the line doubling shows that there exist two distinct velocity fields, for which the velocity difference is directly related to the shock amplitude. As shown on Figs. 1, 3 and 4, the post-shock velocity is negative. Therefore, for the observer, (Eulerian coordinates), the shock is falling down. Thus, the Eulerian velocity of this receding front is smaller than that of the layers.

This is shown by comparing the velocity related to both Hα and Si III line formation regions. Fig. 6 represents the heliocentric radial velocity curve associated to Si III as a function of that associated to the Hα line.

Since loops develop in this diagram, a phase lag exists between the considered line formation regions. Namely, as already mentioned in the previous section, the variation of Hα is late compared to that of Si III. This Van Hoof effect is interpreted in terms of outward propagating wave (Mathias & Gillet 1993). Therefore, if the Hα line formation region is located above that corresponding to the Si III one, the wave propagates outward. Thus, although the shock is falling down within the atmospheric layers, it propagates outward in mass (Lagrangean coordinates). This means that the shock front comes close more and more to the Hα layer during the infalling motion of the atmosphere. This shock, which will be called the "infalling shock", desappears before the end of the ballistic motion of the atmosphere, depending of its intensity.

Then, a rapid expansion phase takes place during the second velocity discontinuity. Shortly before this phase, the atmosphere is nearly at rest. Suddenly, the profile becomes strongly distorted. Despite no visible line doubling, the line shows a well marked asymmetry. This infers that a shock wave, originating from the subphotospheric regions, sweeps the layer outward such as in the classical Schwarzschild (1954) mechanism. This wave is likely caused by the iron opacity κ-mechanism which has been recently shown as the true engine of the pulsation of β Cephei stars. Note that, as for the infalling shock, the Van Hoof effect is also detected here and have the same interpretation.

Thus, the first discontinuity and the associated infalling shock would be a consequence of the wave induced by the κ-mechanism. This second shock will be called the "outward-shock". We could not determine any appreciable differences between the velocity separation between the two components for both lines considered, implying that the shock energy, in the framework of the precision of our data, remains almost constant during its propagation from Si III to Hα layers.

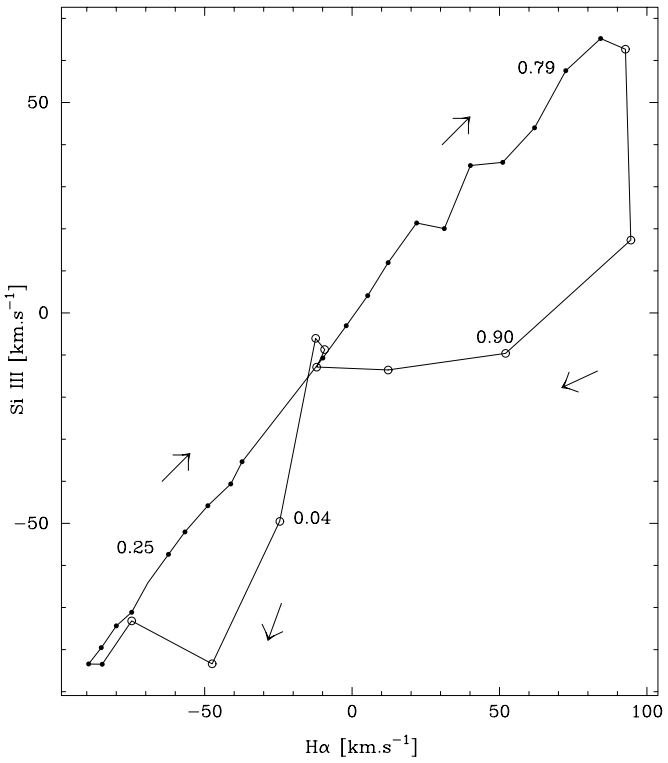

Fig. 6. The radial velocity of Si III is represented versus that of Hα for the night August 1st, 1994. Note that these velocities are associated to the blue component for both lines. Black dots represent the ascending branch of the heliocentric velocity curves while the open circles stand for the descending branch. The arrows indicate the way the loops are drawn (clockwise), whereas the numbers give the pulsation phase of the closest point.

Having this scenario in mind, it is now interesting to consider the stillstand. Indeed, if the upper atmosphere was completely stopped by the denser bottom layers and before the arrival of the outward shock, the stillstand would be at the systemic velocity of the star. However, it is well known that the stillstand is variable in shape (Odgers 1955). Our data show for the two considered nights, that, immediatly after the infalling-shock, from the beginning of the stillstand, the velocity is slightly below the γ-axis, which represents an expansion phase (Figs. 2a and b and 5a and b). This can be interpreted as a bounce on the photospheric layers. From both figures, the larger the intensity of the infalling-shock, the larger the bounce. Then, because gravity acts, the atmosphere slows down and then falls back toward the photosphere, as shown by the velocity value above the γ-axis. This is well shown by the small and continuous decrease of the velocity during the 3/4 of the stillstand phase. In this view, the stillstand can be considered as the final damping step of the infalling atmospheric motion. Its variable shape is the consequence of different amplitudes of the ballistic motion which must changes from cycle to cycle. Indeed, as noted in the previous section, although the above scenario is valid for both studied nights, the line profiles and the velocity curves do not present the same pattern. This may be due to a different intensity of the successive shocks.

5. Conclusion

This study well confirms the presence of two shocks during one pulsation cycle in BW Vul. Dynamically, the "basic" shock (outward-shock) is due to a wave propagating from the subphotosphere, probably initiated by the iron κ-mechanism recently found in these stars. The velocity jump is between 80-100 km.s^{-1} depending on the night. Considering a sound speed of about 15 km.s^{-1} within the Si III/Hα line formation regions, this leads to a Mach number around 5-7. It should be noted that the infalling motion is almost finished when the outward shock occurs during the first night, while during the second night, the velocity jump is again around 40 km.s^{-1}. This shock gives an appreciable outward impulsion to the atmosphere, which is not physically detached from the "unperturbed" photosphere, contrary to the Odgers' scenario (1955) The atmosphere then follows a ballistic motion until it falls back. When the increasing density decelerates the layers, it appears a positive velocity gradient between the bottom and the top of the atmosphere, caused by the increasing density of the gas. When the velocity gradient is large enough, the wave front breakes into an infalling shock for the observer. The maximum front velocity is quite large (between 120-180 km.s^{-1} depending on the night). Thus, during its final acceleration phase ($\varphi = 0.93$), its Mach number is close to 8-12, i.e. this shock is hypersonic contrary to the outward shock. This interpretation is opposite to the one given by Crowe & Gillet (1989) who invoked a second κ-mechanism. Finally, due to inertia, the atmosphere bounces on the photosphere and falls back again until complete damping: this explains the stillstand. It should also be noted that turbulence may play a non-negligeable role which may contribute to line broadening.

This scenario is based on a pure mechanical consideration. However, as noticed by a few authors (e.g. Young et al. 1981), effects of radiative transfer due to changes in the continuous opacity can lead to erroneous interpretations of atmospheric motions. Furthermore, Moskalik & Buchler (1994), using a full self-consistent hydrodynamic model of BW Vul, show that a unique shock wave, originating at the bottom of the He^+ zone, is present during a pulsation cycle and causes the stillstand. This shock produces a sudden jump in the optical depth which contributes to the formation of the apparent discontinuity. However, although the amplitude of their radial velocity curve is correct, the stillstand has a velocity of about -100 km.s^{-1} in the stellar rest frame, which has never been observed for this star.

A future interesting test would be to synthetize line profiles along one cycle using a self-consistent pulsating *atmospheric* model such as the one developed by Fokin (1992) for RR Lyrae stars. This would represent the next step of this work.

Acknowledgements. The authors thank E. Chapellier for a critical reading of the manuscript and helpful suggestions.

References

Aerts C., 1996, A&A 314, 115
Aerts C., Mathias P., Van Hoolst T. et al., 1995, A&A 301, 781
Baranne A., Queloz D., Mayor M. et al., 1996, A&AS 119, 373
Cox A.N., Morgan S.M., Rogers F.J., Iglesias C.A., 1992, ApJ 393, 272
Crowe R., Gillet D., 1989, A&A 211, 365
Dziembowski W.A., Pamyatnykh A.A., 1993, MNRAS 262, 204
Fokin A.B., 1992, MNRAS 256, 26
Kubiak M., 1978, Acta Astron. 28, 153
Mathias P., Gillet D., 1993, A&A 278, 511
Moskalik P., Buchler J.R., 1994, in: Pulsation, Rotation an Mass Loss in Early-Type Stars, Eds. L.A. Balona, H.F. Henrichs & J.-M. Le Contel, Kluwer Academisch Publishers, p. 19
Odell A.P., 1981, ApJ 246, L77
Odell A.P., 1994, IBVS 4138
Odgers G.J., 1955, Publ. Dom. Astrophys. Victoria 10, No 9, 215
Schwarzschild M., 1954, in: Transactions of the IAU VIII, Ed. P.Th. Oosterhoff, Cambridge University Press, p. 811
Young A., Furenlid I., Snowden M.S., 1981, ApJ 245, 998